Shell Theory-Based Estimation of Local Elastic Characteristics of Biological Cells

Elizaveta S. Drozd, Gennadi I. Mikhasev, Marina G. Botogova, Sergei A. Chizhik and Maria E. Mychko

Abstract The shell theory-based approach for the elastic analysis of biological cells is proposed. This approach introduces the estimation of the local Young's modulus of the single cell on the basis of the shell theory and data of the atomic force microscopy (AFM). This method is applicable to evaluate the elastic properties of the cell membrane which stretched under action of the atomic force microscope indenter (AFMI). The cell is represented by a thin shallow spherical shell experiencing the concentrated outward force. The influence of cytoskeleton on the cell deformation is disregarded. Taking into account microscopic sizes of the cell and the indenter tip, the internal nanoscale parameter is introduced into the constitutive equations. On the basis of the experimental data and developed shell model we give a rough estimate of local Young's modulus for the red blood cell.

1 Introduction

Mechanical properties are fundamental characteristics of cells and tissues. They define a number of cytophysiological and cytopathological processes. The cell mechanical parameters may be used as certain markers of various pathologies

---

E.S. Drozd (✉) · S.A. Chizhik · M.E. Mychko
Heat and Mass Transfer Institute of National Academy of Sciences of Belarus,
Brovki St. 4, 220072 Minsk, Belarus
e-mail: drozd.elizaveta@gmail.com

S.A. Chizhik
e-mail: chizhik_sa@tut.by

M.E. Mychko
e-mail: akumananoda@gmail.com

G.I. Mikhasev · M.G. Botogova
Belarusian State University, Nezavisimosti Ave 4, 220030 Minsk, Belarus
e-mail: mikhasev@bsu.by

M.G. Botogova
e-mail: botogova@tut.by

[23, 32]. The study of elastic properties allows us to obtain new knowledge on the biological cells and is also of clinical interest.

There are several methods to evaluate the elastic properties of the biological cells: micropipette aspiration [15, 18, 27, 31, 33], filtering [3, 34], fluctuations of the cell's shape [4, 42], the cell deformation (created by shear stress) by ektocytometer, optical channel or microplates [7, 18, 20], and micromanipulation (optical and magnetic tweezers, magnetic twisting cytometry) [5, 22, 24, 43]. However, the most modern and accurate approach developed during the last decade is the one based on the technology of the atomic force microscopy (AFM) including the force spectroscopy [10, 11, 28, 35, 37–40]. This method allows to determine the value of the local modulus as a result of the indenter impact (AFM probe) on the test material. It should be however noted that the study of biological objects by using any approach is very complicated procedure. It includes the following obligatory steps: preparing samples by a special way, optimizing the measurement parameters and reliable interpreting the experimental results. Analysis of the available literature on the estimation of the cell mechanical properties displays a significant scatter in experimental data obtained by using the AFM. First of all, this fact can be explained by the lack of uniformity in measurements and hence makes the quantitative analysis and comparison of the results to be rather complicated [21, 41]. Secondly, when studying the surface layer of a single cell (with thickness varying from several nanometers to some hundred nanometers) with the AFM methods, we deal with a composite material, the mechanical properties of which are mainly conditioned by the properties of the cortical actin cytoskeleton, two- or three-dimensional network from natural biopolymers (proteins) [41]. And the cytoskeleton structure reorganization results in changing the mechanical properties of cells. In our opinion, the satisfactory results may be reached by developing the realistic continuum mechanical model describing a response of the biological cell on the microscopic indenter.

There are different mechanical models, including the shell ones, which are applied for the mechanical characterization of living cells (e.g., see the survey paper by [25]). Within the shell model, cells are often assumed to have a spherical shape. For instance, [44] developed the spherical shell model to describe motion of the bacteria (cocci) in an ultrasonic field. Recently, [36] studied aspiration of spherical cells represented by a hyperelastic isotropic momentless spherical shell, and the simplified spherical shell model for estimation of the local Young's modulus of erythrocyte on the basis of the AFM data was proposed by [12].

The basic goal of this study is to create the reliable shell theory-based model describing a deformation of the biological cell when subjected to the concentrated adhesion forces. Taking into account microscopic sizes of the cell and the indenter tip, we aim to derive an equation for the shell deflection including the nanoscale effects. Using the experimental data of the nanoindentation, it is possible to obtain the force curve by recording the cantilever deflection while the tip is in contact with the biological body. Among all conditions of the cell-indenter interactions, the regime of adhesion between the indenter tip and cell will be considered. Under this type of interaction (when the action of normal force is directed outwards), the cell membrane is only stretched. In this case the influence of the cytoskeleton on the

strain-stress state of the cell represented by an elastic shell will be negligible and may be disregarded [12].

2 Methods

2.1 Force Spectroscopy Method

The procedure of force spectroscopy constitutes a standard mode of the AFM. The method consists in the realization of the contact deformation of a specimen using the probe and in quantifying the relationship between probe interaction force and distance [6]. We record the cantilever deflection as the sample moves up, reaches the tip and is retracted. The force curve is obtained by monitoring the movement of the reflected laser beam from the rear of the cantilever. The force curves are the relation between the bend of the cantilever and the position of the probe. Knowing the displacement of the sample in the vertical direction and the amplitude of cantilever bending, one can calculate both the resulting deformation of the sample and the total external force that has been applied to it. The force curve is applied to the calculation of Young's modulus (Fig. 1).

Figure 1 shows the different stages of the indentation process. At the beginning of the force curve recording, the tip is distant from the sample and approaches, but does not contact it (a). Since there is no contact the cantilever deflection is constant. As soon as the tip actually touches the sample, the cantilever moves upward (b). Further, as the tip indents the sample, the cantilever arm moves downward (c). The sample is then retracted displaying a reverse behavior to action (c), as indicated by the curve (d) which shows the deflection during retraction. However, when adhesion between sample and tip occurs, the tip will adhere to the sample beyond the point of contact (e), until it finally breaks free again and the deflection returns to zero (f). It should be noted that the approach curve exactly retraces the pathway to point (e) provided there is no piezohysteresis.

We are able to quantify the local elastic properties of a living cell using the force spectroscopy mode. The force curve is obtained by recording the cantilever

Fig. 1 Regime of static force spectroscopy: typical force curve
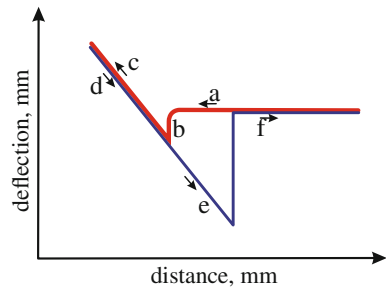
deflection as the tip is brought into contact at the fixed point and then retracted. The Young's modulus may be calculated using the Hertz model describing the elastic deformation of two bodies in contact under load [17]. When applying the Hertz model the indented sample is assumed to be extremely thick in comparison to the indentation depth. In this case the elastic modulus may be calculated as described earlier [9, 23]. Alternatively, the shell theory will be developed to describe the regime of adhesion of a cell with the indenter tip; in this case the cell thickness will be assumed to be very thin with respect to the characteristic size of a cell.

2.2 Shell Theory-Based Model

As mentioned above, a thickness of the biological cell varies in the interval from several to hundreds nanometers, and its characteristic size is a value of about several millimeters. For instance, for the red blood cell the average values of these parameters are $h \approx 10\,\text{nm}$ and $R \approx 2\,\mu\text{m}$ respectively. So, when ignoring the internal cytoskeleton, a cell may be represented by a thin-walled elastic structures. Here, we consider the case of adhesion between the cell and indenter. Note that the radius of indenter (about 40 nm) is much less than the characteristic size of the cell. Then, at small magnitudes of the adhesion forces acting from the indenter tip, in a vicinity of the contact point the cell may be modeled by a shallow spherical shell.

Let R be the radius of the spherical shell representing the cell in a vicinity of the contact point, E the local Young's modulus, and ν Poisson ratio of the material. The midsurface is referred to the orthogonal rectangular coordinate system $\overline{x} = R_c x$, $\overline{y} = R_c y$, where x, y are dimensionless coordinates. The shell is assumed to be under action of the concentrated normal outward force Z.

Taking into account microscopic sizes of the cell and a nanoscopic radius of the indenter tip, we aim in passing to study the influence of the nanoscale effect on deformations of the microscale object. With that end in view, we apply the nonlocal version of elasticity pioneered by [13, 14]. Let σ_{ij} and $\sigma_{ij}^{(m)}$ be microscopic and macroscopic stresses in the shell, respectively. According to the nonlocal elasticity theory, these stresses are linked as follows

$$\mathcal{E}\sigma_{ij} = \sigma_{ij}^{(m)}, \tag{1}$$

where $\mathcal{E}$ is the appropriate linear differential operator which takes into account the effect of the elastic nonlocality. For the two-dimensional strain-stress state it is written as [14]

$$\mathcal{E} = 1 - \left(\frac{e_0 a}{R_c}\right)^2 \Delta, \tag{2}$$

where Δ is the Laplace operator in the dimensionless coordinate system x, y, a parameter e_0 is the material dimensionless constant of nonlocality, and a is the internal characteristic length of the material. For instance, [13] gives the value $e_0 = 0.39$, and for discreet nanoscale structures such as carbon nanotubes, the parameter $a = 0.142$ nm is chosen to be the length of the C-C bond. As concerns biological cells, the parameter $e_0 a$ remains indefinite. So, studying the mechanical behaviors of protein microtubules, [16] varied the small scale parameter $e_0 a$ from 0 to 70 nm.

To describe small deformations of the spherical shallow shell under action of the normal concentrated force we apply the theory of [30] which takes into account the transverse shears. According to this theory, the governing equation, with Eqs. (1) and (2) in mind, may be rewritten as follows

$$\left(\frac{1}{R_c^2}\Delta + \frac{2}{R^2}\right)\left[D\left(\frac{1}{R_c^2}\Delta + \frac{1+v}{R^2}\right)w - \frac{1}{R}\left(1 - \frac{h^2}{5(1-v)R_c^2}\Delta\right)\Phi\right]$$

$$= \left[1 - \frac{(2-v)h^2\Delta}{10(1-v)R_c^2}\right]\Xi\, Z(x, y), \tag{3}$$

$$\left(\frac{1}{R_c^2}\Delta + \frac{2}{R^2}\right)\left[\frac{1}{Eh}\left(\frac{1}{R_c^2}\Delta + \frac{1-v}{R^2}\right)\Phi + \frac{w}{R}\right] = \frac{-v}{2ER_c^2}\Delta\Xi\, Z(x, y),$$

where $D = Eh^3/[12(1-v^2)]$ is the flexural rigidity of the shell, w is the normal deflexion, and Φ is the stress function.

As opposed to equations for macro-scale shells [26, 30], the modified Eq. (3) contain the additional operator Ξ (the derivation of similar equations for nano-scale shells may be found in the paper by [29]) influenced by the nonlocal parameter e_0.

To eliminate the influence of boundary conditions, we assume that the shell is infinite in all directions. Then the concentrated force $Z(x, y) = P\delta(x, y)$ applied in the point $x = 0$, $y = 0$ may be presented by the Fourier integral

$$P(x, y) = \frac{P}{\pi^2}\int_0^\infty \int_0^\infty \cos\alpha x \cos\beta y\, d\alpha d\beta, \tag{4}$$

where $\delta(x, y)$ is the delta function.

The unknown functions from Eq. (3) may be also presented as

$$w(x, y) = \int_0^\infty \int_0^\infty w_{\alpha\beta}(\alpha, \beta)\cos\alpha x \cos\beta y\, d\alpha d\beta,$$

$$\Phi(x, y) = \int_0^\infty \int_0^\infty \Phi_{\alpha\beta}(\alpha, \beta)\cos\alpha x \cos\beta y\, d\alpha d\beta. \tag{5}$$

Substituting Eqs. (4) and (5) into Eq. (3) , and performing the Fourier inversion, one obtains

$$w = \frac{P R_c^2}{\pi^2 D} \int\limits_0^\infty \int\limits_0^\infty K_1 \left[1 + \frac{(e_o a)^2}{R_c^2}(\alpha^2 + \beta^2)\right] \frac{\cos \alpha x \cos \beta y \, d\alpha \, d\beta}{(\alpha^2 + \beta^2 - 2k_R) F(\alpha, \beta)}, \quad (6)$$

where

$$K_1 = \left[(1 + (\eta - \varepsilon)(\alpha^2 + \beta^2))(\alpha^2 + \beta^2 - (1 - v)k_R)\right.$$
$$\left. - \bar\varepsilon(1 + \eta(\alpha^2 + \beta^2))(\alpha^2 + \beta^2)\right]$$
$$F(\alpha, \beta) = \left[\alpha^2 + \beta^2 - k_R)^2 + 4\kappa^4(1 + \eta(\alpha^2 + \beta^2))\right],$$
$$4\kappa^4 = \frac{E h R_c^4}{R^2 D} = \frac{12(1 - v^2) R_c^4}{R^2 h^2}, \quad (7)$$
$$\bar\varepsilon = \frac{vh}{2R}, \quad \varepsilon = \frac{vh^2}{10(1 - v)R_c^2}, \quad \eta = \frac{h^2}{5(1 - v)R_c^2}$$

The characteristic size may be chosen as follows

$$R_c = \frac{\sqrt{Rh}}{\sqrt[4]{12(1 - v^2)}}. \quad (8)$$

Then, proceeding to the polar coordinate system by equations

$$\alpha = \gamma \cos \varphi, \quad \beta = \gamma \sin \varphi, \quad x = r \cos \theta, \quad y = r \sin \theta, \quad (9)$$

one gets

$$w = \frac{P R_c^2}{2\pi D} \int\limits_0^\infty K_2(\gamma) \left[1 + \frac{(e_o a)^2}{R_c^2}\gamma^2\right] \frac{J_0(\gamma r) \gamma \, d\gamma}{(\gamma^2 - 2k_R) F(\gamma)}, \quad (10)$$

where $J_0(\gamma r)$ is the zeroth-order Bessel function of the first kind, and

$$K_2 = \left[(1 + (\eta - \varepsilon)\gamma^2) - (\gamma^2 - (1 - v)k_R) - \bar\varepsilon(1 + \eta\gamma^2)\gamma^2\right],$$
$$F(\gamma) = (\gamma^2 - k_R)^2 + \eta\gamma^2 + 1, \quad k_R = \frac{1}{\sqrt{12(1 - v^2)}} \frac{h}{R}. \quad (11)$$

Since $h^2/R_c \ll 1$ and $k_R \ll 1$, then the term $(1 + k_R^2 + 2\eta k_R)^{-1}$ can be neglected, and

$$\frac{1}{F(\gamma)} \approx \left[1 - \frac{\gamma^2}{1 + \gamma^4}(\eta - 2k_R)\right] \frac{1}{1 + \gamma^4}. \quad (12)$$

Performing simple transformations of functions under the integral (see details in the paper by [26]), one gets the final equations for the normal displacement of the shell subjected to action of the concentrated normal force P:

$$w = w^* + w^{**}, \tag{13}$$

where

$$w^* = \frac{PR_c^2}{2\pi D} \left\{ -\text{kei}(r) - k_R \left[(1+v)\left(\frac{\pi}{2}Y_0(r\sqrt{2k_R}) + \text{ker}(r)\right) + \frac{1}{2}r\,\text{ker}'(r) \right] \right.$$
$$\left. + \left[(\eta - \varepsilon)\,\text{ker}(r) + \frac{\eta}{4}r\,\text{ker}'(r) \right] \right\} \tag{14}$$

is the term obtained earlier for a macro-scale shell [26] and

$$w^{**} = \frac{P(e_o a)^2}{2\pi D} \left\{ \text{ker}(r) + \text{kei}(r)\left[\eta(2 - \bar{\varepsilon}) - \varepsilon - k_R(3 + v) \right] \right\} \tag{15}$$

is the new summand taking into account the nano-scale effect. In Eqs. (14) and (15), $\text{kei}(x)$ and $\text{ker}(x)$ are the Kelvin functions.

Although Eqs. (14) and (15) have singularity in the point $r = 0$, they can be applied for estimation of the maximum displacement of the shell for the case when the force P is distributed over the surface of a small circle of the radius c. When taking into account properties of the Bessel and Kelvin functions, one has

$$w_0 = w_0^* + w_0^{**}, \tag{16}$$

where

$$w_0^* \approx \frac{PR\sqrt{12(1 - v^2)}}{Eh^2\pi} \left[\frac{1}{2c^2} + \frac{1}{2c}\,\text{ker}'(c) - \frac{1}{2}k_R(1+v)\ln\sqrt{2k_R} - \frac{k_R}{4} \right]$$
$$+ \frac{3P}{5\pi Eh}(1+v)(2-v)\left[\text{ker}(c) + \frac{c\,\text{ker}'(c)}{2(2-v)} \right], \tag{17}$$

$$w_0^{**} \approx \frac{P(e_0 a)^2}{2\pi D} \left\{ \text{ker}(c) - \left[\frac{1}{c^2} + \frac{1}{c}\,\text{ker}'(c) \right]\left[\eta(2-\bar{\varepsilon}) - \varepsilon - k_R(3+v) \right] \right\}. \tag{18}$$

Equation (17) have been derived by [26], and term (18) taking into account the scale effect is the new one.

3 Determination of Contact Area

Let c^* be a radius of the contact area between the cell and tip. This contact is provided by the forces of adhesion under withdrawal of the tip out of the cell. It should be noted that a parameter c^* is hardly measurable one during an experiment. When the indenter being taken out the sample, the contact area decreases so that it is very difficult to fix and quantify a radius c^* in the moment of detachment of the tip.

Another available way to determine the contact area is based on the theory of [19]. Let $\Delta\Gamma$ be the surface energy of the sample. This energy is acquired as result of the surface forces appearing in the sample due to cohesion between the sample and tip. According to this theory the contact area is defined by the following equation

$$c^* = \sqrt[3]{R_t K \left(P + 3\pi R_t \Delta\Gamma + \sqrt{(3\pi R_t \Delta\Gamma)^2 + 6\pi R_t \Delta\Gamma P} \right)}, \qquad (19)$$

where

$$K = \frac{3}{4} \left(\frac{(1-v^2)}{E} + \frac{(1-v_t^2)}{E_t} \right), \qquad (20)$$

R_t is the tip radius, E_t, v_t are the Young's modulus and Poisson's ratio of the tip. Since $E \ll E_t$, it is assumed $K \approx 3(1-v^2)/E$ in what follows.

If the surface forces are neglected ($\Delta\Gamma = 0$), then Eq. (19) is transformed into the Hertz formula

$$c^* = \sqrt[3]{P R_t K}. \qquad (21)$$

When the sample is stretched, then the force $P = -P_s$ ($P_s > 0$) is negative. Increasing the force magnitude P_s results in decrease of the contact area (radius c^*). Detachment of the indenter tip from the cell takes place when the magnitude of the stretching force reaches the value

$$P_s = \frac{3}{2} \pi R_t \Delta\Gamma. \qquad (22)$$

Then the surface energy of the cell is as follows;

$$\Delta\Gamma = \frac{2 P_s}{3\pi R_t}. \qquad (23)$$

Substituting Eq. (23) into Eq. (19) results in the following equation for the contact area radius

$$c^* = \sqrt[3]{\frac{3 P_s R_t (1 - v^2)}{4E}}, \tag{24}$$

which will be used in our subsequent calculations.

4 Estimation of Local Young's Modulus

Let $w_{\max}$ be the maximum deflection of the sample in the moment of its detachment from the cantilever. The parameters $w_{\max}$, P_s are assumed to be known ones; they are quantified during an experiment. Returning to the shell theory, we assume that $w_{\max} = w_0$, where w_0 is defined by (16)–(18); the function w_0 depends on the external force P_s, the local Young's modulus E, thickness h and the dimensionless radius c of the contact area. Taking into account Eq. (24), one obtains the following equations

$$w_{\max} = w_0[P_s, E, h, c(P_s, E)], \quad c = c^*/R_c \tag{25}$$

with respect to the modulus E.

We have performed series of the AFM probes and computations for the red blood cell at the following parameters: $R_t = 40$ nm, the shell radius $R = 2\,\mu$m (the total radius of the red blood cell in the point of indentation [8], Poisson ratio $v = 0,5$ [1, 2], $e_0 a = 0$. The shell thickness h was initially taken to be equal to 10 nm, which corresponds to the average thickness of the cell membrane (without its cytoskeleton). Solving Eq. (25) at different values of parameters P_s, $w_{\max}$ (the quantified maximum displacements $w_{\max}$ were varied in the interval from 10–100 nm), we compared the obtained values of E with data found by the Hertz model.

Figure 2 shows the diagrams for average values of Young's modulus (in relative units) at different deformations of the cell.

The diagrams marked by blue were constructed by using both the Hertz model and data of nanoindentations of the sample (at $w_{\exp} > 0$), and the diagrams in red correspond to data found from the shell model and experimental data by stretching the sample (at $w_{\exp} < 0$). All magnitudes shown in this figure as well as in others were found by averaging data of a whole number of indentations and adhesive tensions of the sample, then the average values were normalized by the magnitude $E = 338.5$ kPa. As result of linearity of the shell model, the shell-based values E_{sh} do not depend on the displacement $w_{\exp}$. However, the Hertz model demonstrates very strong dependence on $w_{\exp}$: increasing the sample deformation results in decrease of the local modulus E_H. It may be seen that both models give close results for very small deformations. Considerable gap in results at large values of $|w_{\exp}|$ can be explained by influence of both the cell internal components and compressive strains

Fig. 2 Local Young's
modulus in relative units
versus the sample
displacement w_{max} found by
the shell and Hertz models
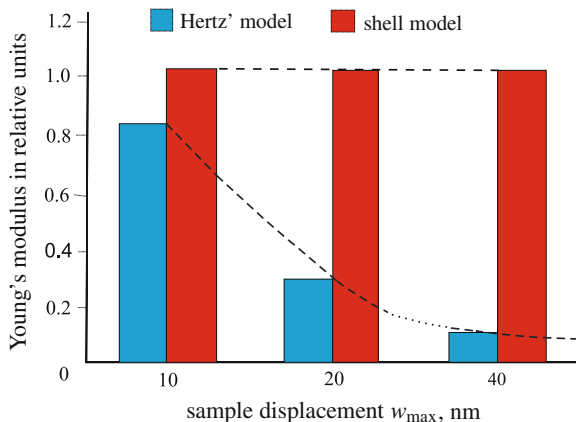
(when using Hertz model). As concerns the shell model, it is linear and can not be
used for prediction of large deformations. In addition, applying the shell model for
the stretched cell we ignored the cell cytoskeleton. It should be also noted that a
value of E found at large displacements of the sample can not be considered as local
Young's modulus of a cell; most probably it might be interpreted as the effective
stiffness of all structure of the microscopic biological object.

It is obvious that the mechanical properties of a cell is influenced by its internal
components (cytoskeleton). The cytoskeleton consists of a dense three-dimensional
network of filaments. Among them it is possible to distinguish at least three types:
microtubules, microfilaments and intermediate filaments. They provide mechanical
stability of the surface layer of cytoplasm and create conditions that allows for the cell
to change its shape and move. Filaments have sufficient resistance to bending in large
scales and remarkable resiliency in small scales [16]. The thickness of microtubules
is approximately 24 nm, the thickness of microfilaments (f-actin) is about 5–8 nm and
the intermediate filaments diameter is 8–10 nm [8]. The thickness of a cell membrane
is stated to vary from 3 to 11 nm. Thus, the overall thickness of a cell membrane and
neighboring elements of the cytoskeleton is in the range about 10–40 nm. To take
into account the influence of the cytoskeleton on the elastic properties of a cell, we
introduced into the shell model the effective thickness which was varied in the range
mentioned above. Numerical calculations by Eq. (25) performed at $P_s = 0.1$ nN,
$w_{exp} = 10$ nm revealed that increasing the shell thickness h from 10 nm to 40 nm
leads to near tenfold decrease of the local Young's modulus (from 338–34 kPa).

The next question that we are interested in: is there such equivalent shell thickness
at which Young's modulus calculated by using both models are close? Coincidence
of moduli would determine the degree of participation of the cellular component in
the processes of compression and stretching. The results of this evaluation are shown
in Fig. 3. It may be seen that the values of the local elastic modulus estimated on
the basis of the shell and Hertz models are close to each other when the maximum
sample deformation w_{exp} is near the value of the shell thickness (at $h/w_{exp} \approx 1.15$).
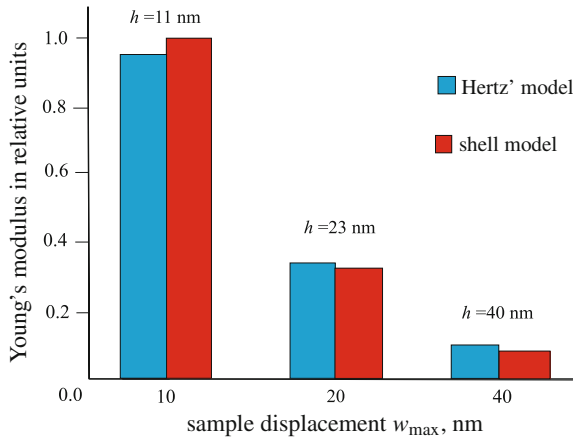
Fig. 3 Local Young's modulus in relative units vs. the sample displacement w_{max} found by the shell and Hertz models at different cell thicknesses $t_1 = 11, 23, 40$ nm

Finally, taking into account the microscopic sizes of the cell and indenter, we attempted to estimate the effect of the internal scale on local properties of the sample. According to the nonlocal theory of elasticity of [13, 14], the principle parameter characterizing the nonlocal effect is the scale coefficient ae_0, where a and e_0 were introduced above. The satisfactory estimation of this parameter for biological micro- and nano-objects is still unsolved problem. For instance, studying behavior of the protein microtubule, [16] varied the small scale parameter ae_0 from 0 to 70 nm. Following [16], we have also performed the series of accurate calculations at different values of ae_0. It was found that impact of the parameter ae_0 on the local modulus E is negligibly small: at $ae_0 = 70$ nm, the additional term (18) gives correction (for E) not exceeding 0.01 %. Very weak influence of the scale parameter ae_0 on the assessment of the modulus E might be explained by large diameter of the indenter (about 40 nm) with respect to the cell size. As shown in the paper by [29], the scale parameter ae_0 should be taken into consideration for prediction of mechanical behavior which is characterized by high variability of deformations along even if one direction on the surface of a nanoscale shell object. In our case, decreasing the area of application of the external force Z would result in increasing variability of the cell deflection in a vicinity of the contact point between the tip and cell. However, utilization of more thin indenter tip for indentation of biological cells generates the following serious problems:

(a) the microscope should be thoroughly standardized;
(b) all probes should be done with very high accuracy;
(c) outcome scatter for different probes becomes more significant;
(d) one rises the risk of the membrane penetration.

In our opinion, further improvement of the shell model for prediction of mechanical properties of biological cells might be done by introducing the cell components

into model. As the first step of this development, the cytoskeleton structure could be represented by an elastic foundation for a shell modeling a cell.

5 Conclusions

The approach for estimation of the local Young's modulus of a biological cell, based on the shell theory and data of the AFM, has been proposed. The developed method is applicable for the case when the cell membrane is stretched by the adhesion forces between the AFMI and sample. When developing the mechanical model, the cell has been represented by a thin elastic isotropic spherical shell with the radius equaled to the total one of the sample in the point of indentation. The differential equations written in terms of the normal displacements and stress function and taking into account the shear deformations and nano-scale effect have been considered as governing ones. In the developed model the internal components of a cell (cytoskeleton) are disregarded. The solution of these equations with the external concentrated force has been constructed using the Fourier transformation. The found solution has been modified for the case of the adhesion forces applied to the small circular area. The radius of the contact area has been defined by the theory of Johnson-Kendall-Roberts. Substitution of this radius into the obtained solution of the governing equations has allowed to derive the transcendental equation with respect to unknown Young's modulus.

The series of the probes for the red blood cell corresponding to conditions of adhesion and indentation as well has been made. The averaged data (the force acting from the AFMI and the maximum displacement of the sample) of these probes have been introduced into the mathematical model. Alternatively, the Hertz theory has been applied to estimate the local mechanical properties of the cell when subjected to the indentation forces.

Comparative analysis of data obtained by using the two approaches allows to conclude:

- both models give close results only for very small deformations of the cell (about 10 nm) and at the effective cell thickness having the order of the maximum deflexion of the sample;
- introducing the nano-scale parameter into the mechanical model does not give some noticeable correction for the local Young's modulus found at the generally accepted size of the indenter tip (about 40 nm);
- more accurate estimations of the local mechanical properties of a cell might be done by incorporation of the cell components into the mechanical model; influence of the cytoskeleton could be taking into account by introducing the nonhomogeneous elastic foundation into the shell model.

References

1. A-Hassan, E., Heinz, W., Antonik, M., D'Costa, N., Nageswaran, S., Schoenenberger, C., Hoh, J.: Relative microelastic mapping of living cells by atomic force microscopy. Biophys. J. **74**(3), 1564–1578 (1998)
2. Alcaraz, J., Buscemi, L., Grabulosa, M., Trepat, X., Fabry, B., Farré, R., Navajas, D.: Microrheology of human lung epithelial cells measured by atomic force microscopy. Biophys. J. **84**(3), 2071–2079 (2003)
3. Baerlocher, G., Schlappritzi, E., Straub, P., Reinhart, W.: Erythrocyte deformability has no influence on the rate of erythrophagocytosis in vitro by autologous human monocytes/macrophages. Br. J. Haematol. **86**(3), 629–634 (1994)
4. Baumann, M.: Cell ageing for 1 day alters both membrane elasticity and viscosity. Pflugers Arch. **445**(5), 551–555 (2003)
5. Berrios, J., Schroeder, M., Hubmayr, R.: Mechanical properties of alveolar epithelial cells in culture. J. Appl. Physiol. **91**(1), 65–73 (2001)
6. Burnham, N., Colton, R.: Measuring the nanomechanical properties and surface forces of materials using an atomic force microscope. J. Vac. Sci. Technol. **A7**, 2906–2913 (1989)
7. Caille, N., Thoumine, O., Tardy, Y., Meister, J.J.: Contribution of the nucleus to the mechanical properties of endothelial cells. J. Biomech. **35**(2), 177–187 (2002)
8. Cherenkevich, S., Martinovic, K.A.G.N.: Biological Membranes. Belarusian State University, Minsk (2009)
9. Chizhik, S., Huang, Z., Gorbunov, V., Myshkin, N., Tsukruk, V.: Micromechanical properties of elastic polymeric materials as probed by scanning force microscopy. Langmuir **14**, 2606–2609 (1998)
10. Costa, K., Sim, A., Yin, F.: Non-hertzian approach to analyzing mechanical properties of endothelial cells probed by atomic force microscopy. J. Biomech. Eng **128**(2), 176–184 (2006)
11. Drozd, E, Chizhik, S.: Estimation of the elastic modulus for highly flexible materials by the method of indentation and separation of a spherical indenter at nanoscale (in Russ.). Natl. Acad. Sci. Reports **54**, 117–122 (2010)
12. Drozd, E., Mikhasev, G., Chizhik, S.: Evaluation of the local elasticity modulus of biological cells on the basis of the shells theory. Ser. Biomech. **27**(3–4), 17–22 (2012)
13. Eringen, A.: On differential equations of nonlocal elasticity and solutions of screw dislocations and surface waves. J. Appl. Phys. **54**, 4703–4710 (1983)
14. Eringen, A.: Nonlocal Continuum Field Theories. Springer, New York (2002)
15. Ewans, E., Waugh, R., Melnik, L.: Elastic area compressibility modulus of red cell membrane. Biophys. J. **16**(6), 585–595 (1976)
16. Gao, Y., Lei, F.M.: Small scale effects on the mechanical behaviors of protein microtubules based on the nonlocal elasticity theory. Biochem. Biophys. Res. Commun. **387**, 467–471 (2009)
17. Hertz, H.: Ueber die Berührung fester elastischer Körper. J für die reine und angewandte Mathematik **92**, 156–171 (1881)
18. Hochmuth, R., Mohandas, N., Blackshear, P.: Measurement of the elastic modulus for red cell membrane using a fluid mechanical technique. Biophys. J. **13**(8), 747–762 (1973)
19. Johnson, K., Kendall, K., Roberts, A.: Surface energy and the contact of elastic solids. Proc. R. Soc. **A324**, 301–313 (1971)
20. Kaneta, T., Makihara, J., Imasaka, T.: An optical channel: a technique for the evaluation of biological cell elasticity. Anal. Chem. **73**(24), 5791–5795 (2001)
21. Kuznetsova, T., Starodubtseva, M., Yegorenkov, N., Chizhik, S., Zhdanov, R.: Atomic force microscopy probing of cell elasticity. Micron **38**(8), 824–833 (2007)
22. Laurent, V., Fodil, R., Cañadas, P., Féréol, S., Louis, B., Planus, E., Isabey, D.: Partitioning of cortical and deep cytoskeleton responses from transient magnetic bead twisting. Annal. Biomed. Eng. **31**(10), 1263–1278 (2003)
23. Lee, G., Lim, C.: Biomechanics approaches to studying human diseases. Trends Biotechnol. **25**(3), 111–118 (2007)

24. Li, C., Liu, K.: Nanomechanical characterization of red blood cells using optical tweezers. J. Mater. Sci. - Mater. Med. **19**(4), 1529–1535 (2008)
25. Lim, C., Zhoua, E., Quek, S.: Mechanical models for living cells - a review. J. Biomech. **39**(2), 195–216 (2006)
26. Lukasiewicz, S.: Local Loads in Plates and Shells. Polish Scentific Publishers, Warszawa (1979)
27. Maggakis-Kelemen, C., Biselli, M., Artmann, G.: Determination of the elastic shear modulus of cultured human red blood cells. Biomed. Tech. **47**(1), 106–109 (2002)
28. Mahaffy, R., Park, S., Gerde, E., Käs, J., Shih, C.: Quantitative analysis of the viscoelastic properties of thin regions of fibroblasts using atomic force microscopy. Biophys. J. **86**(3), 1777–1793 (2004)
29. Mikhasev, G.: On localized modes of free vibrations of single-walled carbone nanotubes embedded in nonhomogeneous elastic medium. Z Angew. Math. Mech. **94**(1–2), 130–141 (2014)
30. Naghdi, P.: On the theory of thin elastic shells. Quart. Appl. Math. **14**, 369–380 (1957)
31. Nash, G., Wyard, S.: Erythrocyte membrane elasticity during in vivo ageing. Biochim. et. Biophys. Acta. **643**(2), 175–269 (1981)
32. Radmacher, M.: Studying the mechanics of cellular processes by atomic force microscopy. Methods Cell Biol. **83**, 91–189 (2007)
33. Rand, R., Burton, A.: Mechanical properties of the cell membrane. I. Membrane stiffness and intracellular pressure. Biophys. J. **4**(2), 115–135 (1964)
34. Rasia, R., Valverde, J., Rosasco, M.: Blood preservation. bacteriological, immunohematological, hematological and hemorrheological studies. Sangre **43**(1), 71–76 (1998)
35. Rosenbluth, M., Lam, W., Fletcher, D.: Force microscopy of nonadherent cells: a comparison of leukemia cell deformability. Biophys. J. **90**(8), 2994–3003 (2006)
36. Rudenko, O., Kolesnikov, A.: Aspiration of a nonlinear elastic spherical membrane. Int. J. Eng. Sci. **80**, 62–73 (2014)
37. Scheffer, L., Bitler, A., Ben-Jacob, E., Korenstein, R.: Atomic force pulling: probing the local elasticity of the cell membran. Europ. Biophys. J. **30**(2), 83–90 (2001)
38. Sirghi, L., Ponti, J., Broggi, F., Rossi, F.: Probing elasticity and adhesion of live cells by atomic force microscopy indentation. Europ. Biophys. J. **37**(6), 935–945 (2008)
39. Smith, B., Tolloczko, B., Martin, J., Grütter, P.: Probing the viscoelastic behavior of cultured airway smooth muscle cells with atomic force microscopy: stiffening induced by contractile agonist. Biophys. J. **88**(4), 2994–3007 (2005)
40. Starodubtseva, M., Chizhik, S., Yegorenkov, N., Nikitina, I., Drozd, E.: Formatex Research Center. Badajoz, chap Study of the mechanical properties of single cells as biocomposites by atomic force microscopy, Microscopy: Science, Technology, Applications and Education Vol. 3, 470–477 (2010)
41. Starodubtseva, M.N.: Mechanical properties of cells and ageing. Ageing Res. Rev. **10**(1), 16–25 (2011)
42. Tishler, R., Carlson, F.: A study of the dynamic properties of the human red blood cell membrane using quasi-elastic light-scattering spectroscopy. Biophys. J. **65**(6), 2586–2600 (1993)
43. Tseng, Y., Kole, T., Wirtz, D.: Micromechanical mapping of live cells by multiple-particle-tracking microrheology. Biophys. J. **83**(6), 3162–3176 (2002)
44. Zinin, P.V., Allen, J.S.: Deformation of biological cells in the acoustic field of an oscillating bubble. Phys. Rev. E **79**, 021 (2009)